Enhanced Colloidal Stability of Al_2O_3-Water Nanofluids Using a Lauryl Sulfate-Based Surface-Active Ionic Liquid as Dispersant

Stephen S. Doliente[a,b*], Glaiza T. Postrado[b], Susan D. Arco[c], Rizalinda L. de Leon[b,d]

[a]*Department of Chemical Engineering, University of the Philippines Los Baños, Laguna 4031, Philippines*
[b]*Energy Engineering Program, University of the Philippines, Diliman, Quezon City 1101, Philippines*
[c]*Institute of Chemistry, University of the Philippines, Diliman, Quezon City 1101, Philippines*
[d]*Department of Chemical Engineering, University of the Philippines, Diliman, Quezon City 1101, Philippines*

Abstract – *Originally intended as alternative thermal fluids, nanofluids or nanosolid-liquid composites now have other emerging industrial applications. However, nanofluids' long-term colloidal stability must be further developed. In this original research, a halogen-free, low cost alkyl sulfate-based surface-active ionic liquid, 1-hexyl-3-methylimidazolium lauryl sulfate ([HMIM]LS) was proposed as a dispersant for Al_2O_3-water nanofluids to enhance its colloidal stability. Colloidal stability of Al_2O_3 nanoparticles dispersed in [HMIM]LS aqueous solution was monitored for one week using UV-vis spectroscopy, zeta potential measurement and particle size distribution. From UV-vis spectroscopy, absorbance of the nanofluid with [HMIM]LS was consistently higher than the controls even until day 7 by a factor of 38. The zeta potential of the nanofluid with [HMIM]LS became more negatively charged from -19.2 mV to -36.7 mV on day 0 and day 7. In spite of these modest values attributed to the adsorbed IL layer on the nanoparticle surface, these results supported the double layer micellar stabilization mechanism. Particle size distribution also corroborated with the absorbance and zeta potential results by showing that larger-sized particles settle slower in the nanofluid with [HMIM]LS compared to the controls. These results showed that [HMIM]LS was an effective dispersant for Al_2O_3-water nanofluids.*

Keywords—Colloidal stability, Nanofluids, Ionic Liquid

I. INTRODUCTION

Since its inception by Choi in 1995, the research and development on nanofluids or the suspension of nanoparticles in conventional fluids like water, oils and glycols has experienced exponential growth [1]. By dispersing nanoparticles (usually <100 nm in size) to conventional fluids, the nanosolid-liquid composites produced have anomalously, highly effective thermal conductivities. Thus, a significant bulk of research on nanofluids has originally been on heat transfer and their thermal science applications [1, 2]. Other emerging applications of nanofluids include enhanced gas absorption [3], media for solar energy harvesting [4], optically active materials for laser production [5], vectors for nanomedicine [6] and media for catalytic reactions [7, 8]. Most of these applications rely on the superior properties of nanofluids such as enhanced effective thermal conductivity, increased heat and mass transport, and remarkable electromagnetic activity. To achieve control over these desired properties, the nanoparticles must remain dispersed indefinitely in the conventional fluids [1, 9].

Generally, nanometre-sized solid particles in fluid suspensions have better colloidal stability over millimetre- and/or micrometre-sized particles. However, the long-term stability of nanofluids still remains a challenge [2, 10, 11]. Colloidal stability refers to a physical state of the system wherein the particles are well-dispersed with little or no particle aggregation, and its level must also be dependable over an extended period of time [12]. Colloidal stability is also an important parameter for the consistency of nanofluids' properties and performance [13].

Conventionally, surfactants or dispersants as additives are used to enhance colloidal stability [2, 10, 11, 14-17]. When dispersants are adsorbed on nanoparticles' surface and form micelles, they increase the contact between the nanoparticles and the base fluid [13]. These adsorbed surfactants provide a repulsive force that prevents particle-to-particle aggregation [10, 11, 16, 17]. Moreover, the addition of surfactants in nanofluids has shown to have enhanced the effective thermal conductivity as noted in several studies [2, 17]. However, the usefulness of common surfactants is limited especially for high-temperature applications [1, 10, 11, 17].

A promising alternative to common dispersants are surface-active ionic liquids (SAILs) [18]. As ionic liquids (ILs), they are thermally (> 350°C, generally) and chemically stable [19, 20]; however, they possess an amphillic nature similar to surfactants due to the presence of long-alkyl chains [18, 21]. A common chemical structure of ILs consists of R,R1-dialklyimidazolium cations (Figure 1) and a wide range of halide or halide-based anions. Since these typical anions pose serious concerns in thermal applications, thus, "greener" ILs are synthesized using halogen-free anions that are environmentally benign [21, 22]. Recently, halogen-free SAILs have been synthesized through anion exchange with sodium lauryl sulfate, which is a natural and low-cost surfactant derived from coconut [18, 22]. This lauryl sulfate-based SAIL possesses superior surface activity (over sodium lauryl sulfate and halogen-anionic SAILs) and well-studied biodegradability [18].

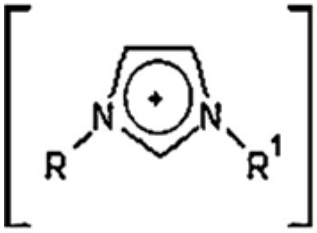

Figure 1. Representation of R,R'-dialklyimidazolium cation structure.

To benchmark SAILs as potential dispersants for a water-based nanofluid, Al_2O_3-water nanofluid is chosen in this study. Using Al_2O_3 or alumina as the nanoparticle takes advantage of its cost-effectivity and ready-availability among engineering ceramics [15]. On the other hand, water is the most commonly used coolant in the industry [17]. Hence, the industrial applications of Al_2O_3-water nanofluid as a thermal fluid is quite promising [23]. From literature search of Al_2O_3-water nanofluids, its stability, properties and applications are well-documented [14, 15, 17, 24]. However, there are limited researches in using SAILS or non-functionalized ILs as alternative dispersants for Al_2O_3-water nanofluids to address the challenges on its long-term colloidal stability.

A related study on the application of a quaternary ammonium-based IL to enhance the solvent extractive capacity of Al_2O_3 suspensions reported uniform particle size through time. This result showed the IL's particle size-controlling and stabilizing capabilities that can potentially benefit nanofluid [25-27]. Most of the studies to date that directly utilized ILs as dispersant were for carbon nanotubes (CNT)-water and gold-water dispersions [26-35]. Gold-water nanofluids involved a one-step method; wherein the gold nanoparticles were synthesized from the reaction between chloroauric acid ($HAuCl_4$) and an acid reductant in the presence of an IL [26-29]. In the studies of [27] and [29], the ILs were demonstrated as stabilizing-agents that prevented particle aggregation through electrostatic and steric hindrance. These results were attributed to the double layer micellar structure formed around the nanoparticles [27]. For CNT-water nanofluids, halogen anionic Gemini- and carbazole-tailed amphiphilic imidazolium ILs had been shown to effectively disperse CNT in water [33, 34]. In addition, Gemini-imidazolium ILs maintained the CNT-water dispersion stability even after one month [33]. Hence, there is a need to intensively investigate the application of ionic liquids, particularly surface-active ones, in enhancing the colloidal stability of water-based nanofluids.

In this study, the enhanced long-term colloidal stability of aluminum oxide (Al_2O_3) in water using a halogen-free, low cost alkyl sulfate-based SAIL, 1-hexyl-3-methylimidazolium lauryl sulfate ([HMIM]LS) as dispersant is reported. To date, there are no similar or related studies that use this SAIL as dispersant to any nanosolid-liquid suspensions. Nevertheless, it was chosen on the basis of its surface activity and solubility in water. The long alkyl chain length rendered the IL with a relatively high surface activity (or relatively low critical micelle concentration (CMC)) [36, 37]; yet, it was completely miscible in water [22]. A conductometric experiment on varying concentrations of [HMIM]LS aqueous solutions was performed to determine its CMC [38]. To achieve the formation of double layer micellar structures, [HMIM]LS concentration was set well above the CMC. Then, the nanoparticle fluid suspension was prepared using [HMIM]LS aqueous solution (at a fixed concentration) as the dispersing medium. Finally, the relative measures of colloidal stability used in this study were UV-vis spectroscopy (in terms of absorbance), zeta potential measurements and particle size distribution monitored over a one-week period. In addition to these quantitative measures, sedimentation over a one-month period was conducted to visually monitor the colloidal stability [10, 11, 16, 17, 39, 40].

II. MATERIALS AND METHODS

2.1 Materials

γ-Aluminum oxide nanopowder was purchased from Sigma-Aldrich Co. LLC, Singapore and used upon receipt. It had an average particle size < 50 nm (TEM) and surface area > 40 m^2/g (BET). [HMIM]LS was synthesized and prepared based on these studies [22, 26, 27]. Ultrapure water prepared by a 4-stage Milli-Pore purification system was used in this study.

2.2 Measurement of the critical micelle concentration (CMC) of [HMIM]LS

Diluted aqueous [HMIM]LS solutions with concentrations ranging from 0.10 to 7.3 mM were prepared. Using two (2) replicates of 10 mL of the solutions, the electrical conductivity of each solution was measured (Conductivity Meter, Eutech) at 25°C (Water Bath, Polyscience). A plot of the average electrical conductivity against [HMIM]LS concentration was used to determine the CMC, which was indicated through the sudden change in the slope of the plot [38]. From the plot, the CMC was estimated from the intersection point of the two lines both fitted with slope-intercept equations.

2.3 Aluminum oxide (Al_2O_3) nanofluids preparation

An aqueous solution of 30 mM [HMIM]LS (blank) was analytically prepared as the nanoparticle dispersing medium. This ionic liquid concentration was 30 times its CMC. Next, Al_2O_3 (12 mg) was added in the dispersing medium (40 mL) to prepare 300 ppm nanofluids for both samples (with IL dispersant) and controls (ultrapure water only). Finally, the suspension was agitated at 280 rpm for two hours (Gyratory Shaker G76, New Brunswick Scientific, USA) and then sonicated at 45 kHz, 100% amplitude and sweep mode for an hour (Ultrasonic Bath D78224, Elma Group, Inc., Germany).

2.4 Relative measures of colloidal stability

The colloidal stability of aluminum oxide (Al_2O_3) nanofluids prepared was evaluated by sedimentation, UV-vis spectroscopy, zeta potential and particle size distribution. For sedimentation, digital photos (Sony Cybershot DSC-W30) were taken on Day 0 (immediately right after their preparation), Day 7 (a week after preparation) and after Day 30 to visually compare the colloidal stability of the samples (300 ppm Al_2O_3 in 30 mM [HMIM]LS) against the controls (300 ppm Al_2O_3 in ultrapure water). While sedimentation provided qualitative data, results from UV-vis spectroscopy, zeta potential measurements and particle size distribution gave quantitative data. These parameters were measured on the samples, controls and blanks (30 mM [HMIM]LS) in triplicates at Day 0. These parameters were measured again on Day 3 (three days after preparation) and Day 7 without additional

agitation and/or sonication prior taking measurements. UV-Vis spectrophotometer (Lambda 850, PerkinElmer, USA) with its quartz cuvettes was used to measure the absorbance from 200 nm to 800 nm. Before each absorbance measurement, dilution was needed to ensure that the reading was well within the detection limit of the instrument. A zetasizer (Malvern Zetasizer Nano Series) was used to simultaneously measure the zeta potential and particle size distribution, wherein no prior dilution was required. The reported value of each of these parameters was the average of triplicate measurements. Moreover, the measurements were done at random to guarantee the statistical validity of the results.

III. RESULTS & DISCUSSION

3.1 Critical micelle concentration (CMC) of [HMIM]LS

For double layer micellar stabilization to take effect, the concentration of [HMIM]LS had to be set above its critical micelle concentration (i.e. CMC is when there is maximum surface coverage of the particle surface) [41]. As an additional challenge, there was no current literature on the CMC of [HMIM]LS. To address this in the current application, CMC was then considered as the minimum concentration at which surfactants form micelles, which was marked by the abrupt changes in transport properties [12]. Using this concept, the CMC of [HMIM]LS was experimentally determined through electrical conductivity measurements against varying concentrations of [HMIM]LS solutions [38].

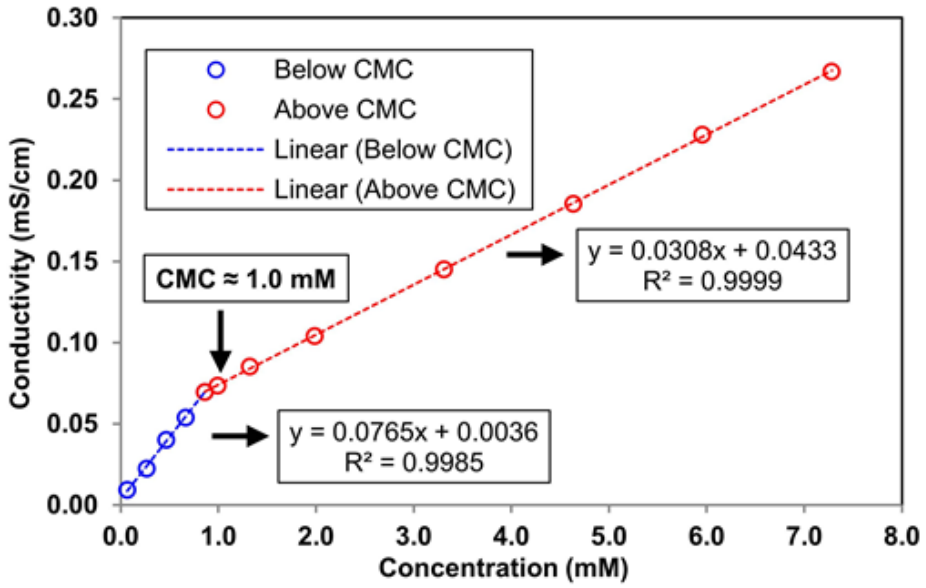

Figure 2. [HMIM]LS critical micelle concentration (CMC) determined from plot of electric conductivity measurement of solutions against their concentration: () electric conductivity measured for concentrations below the CMC, (---) linear fit to electric conductivity as function of concentrations below the CMC, () electric conductivity measured for concentrations above the CMC, and (---) linear fit to electrical conductivity as function of concentrations above the CMC.

Table 1. Analysis of variance: Effect of [HMIM]LS concentration to the electrical conductivity of the solution.

Source	Sum of squares	Degrees of freedom	Mean square	F value	p-value Prob > F	Remark
Model	0.14965	11	0.013605	4531.653	< 0.0001	significant
A-IL concentration	0.14965	11	0.013605	4531.653	< 0.0001	
Pure Error	3.6E-05	12	3E-06			
Cor Total	0.149686	23				
The Model F-value of 4531.65 implies the model is significant. There is only a 0.01% chance that a "Model F-Value" this large could occur due to noise.						

The CMC of [HMIM]LS was found well within the concentration range of interest as shown by the abrupt change in the slope of the plot of electrical conductivity versus concentration (**Figure 2)**. From the linear curve fits, two slope-intercept equations were obtained. Then equating these to find the intersection, the CMC of [HMIM]LS was determined to be 0.8687 mM or approximately 1.0 mM. Analysis of variance on the results showed that they were statistically significant (**Table 1**). Moreover, the R-squared values for the two linear plots of electrical conductivity-concentration approached unity. Based on the results, it can be concluded that the determined CMC was statistically reliable.

In a related study [37], the CMC of the mixture of 1-hexyl-3-methylimidazolium chloride ([HMIM]Cl) and sodium lauryl sulfate (SLS) was measured and found to be ~2.8 mM. Similarly, the dilution range of prepared IL solutions was set near this concentration as well as with the CMC of SLS as the upper limit. However, the CMC measured for the aqueous [HMIM]LS solution in this study was lower by 64% than the CMC for a mixture of [HMIM]Cl and SLS. The CMC measured in that study [37] might have been attributed to sodium (Na^+) and chloride (Cl^-) counterions in a [HMIM]Cl-SLS mixture that can influence the CMC [12]. In this study, [HMIMI]LS in water had only two available ionic species, such that no counterions were present that could influence its CMC. Hence, the low CMC measured for the aqueous [HMIM]LS solution might be largely attributed to the high surface activity of $[HMIM]^+$ due to its long alkyl chain length [18, 21, 36] that favorably led to the formation of micelles with lauryl sulfate even at a low concentration [18, 37].

From the CMC of the [HMIM]LS determined in this study, the solution concentration as medium for the nanofluids prepared was arbitrarily fixed at 30 mM because nanoparticles tend to shift the CMC to higher numerical values [42]. Benchmarked to SLS as surfactant for Al_2O_3-water dispersions, the [HMIM]LS concentration set for this study was well within the concentration range of 10 mM to 50 mM by earlier studies [43-45].

3.2 Sedimentation

Sedimentation is usually the primary method to visually evaluate the dispersion quality of nanofluids [40]. **Figure 3(a)**, **Figure 3(b)** and **Figure 3(c)** showed that the nanofluids with [HMIM]LS remained more dispersed than the controls even after more than a month of evaluation. On the other hand, settling was evident in the controls as shown in **Figure 3(d)**, **Figure 3(e)** and **Figure 3(f)**. On Day 7, most of the nanoparticles in the controls had already settled out. From these qualitative results, the long-term colloidal stability of Al2O3-water nanofluids was improved with the addition of [HMIM] LS as dispersant.

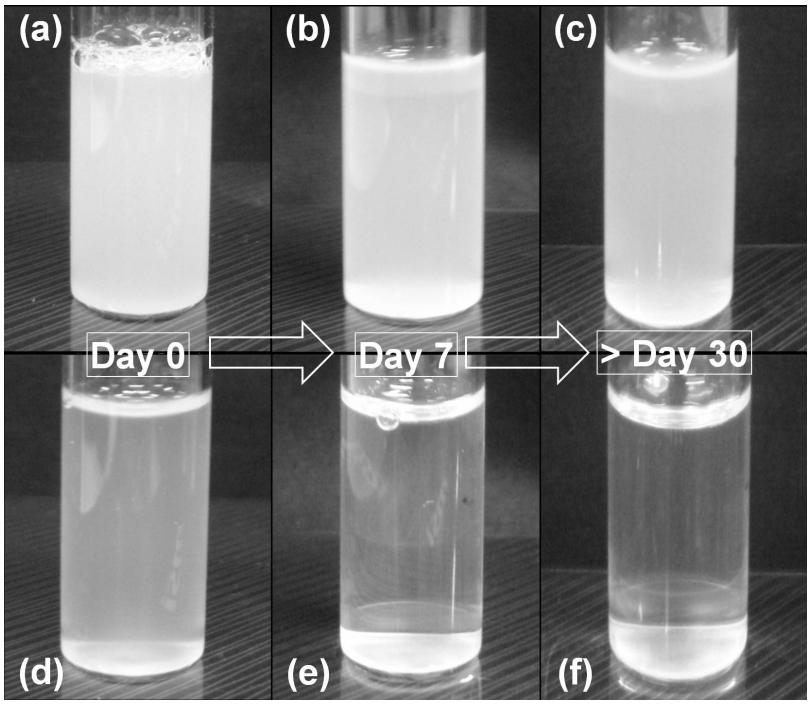

Figure 3. Sedimentation photographs of Al_2O_3-water nanofluids prepared using aqueous solution of [HMIM]LS (a, b, c) and prepared using ultrapure water only (d, e, f), respectively, both showing elapsed time from day 0 to > day 30; nanoparticles were at 300 ppm and concentration of [HMIM]LS was at 30 mM.

3.3 UV-vis spectroscopy

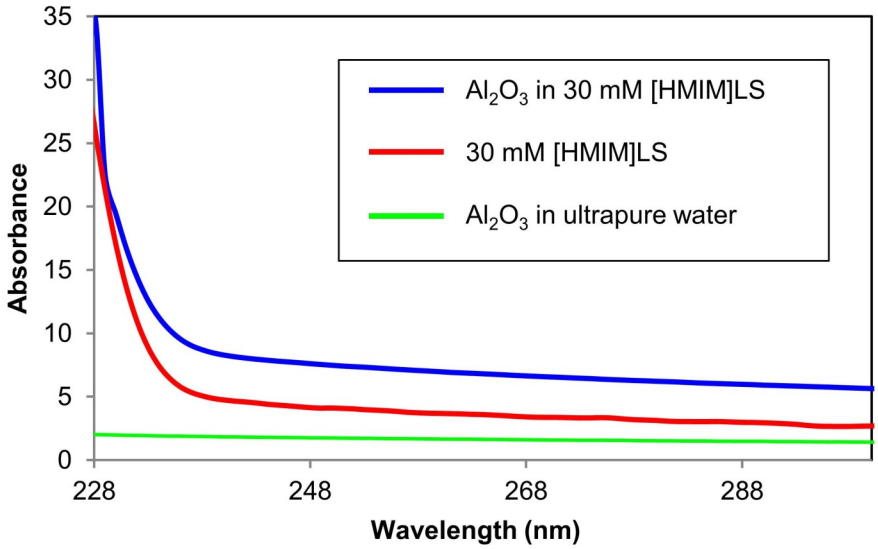

Figure 4. UV-Vis spectra of Al_2O_3 nanofluids and aqueous [HMIM]LS solution: (—) 300 ppm Al_2O_3 in 30 mM [HMIM]LS, 30 mM [HMIM]LS (—), and (—) 300 ppm Al_2O_3 in ultrapure water. Please note that the samples were diluted prior to any absorbance measurements within the detection limit of the equipment; absorbance values presented here were after multiplying the dilution factor.

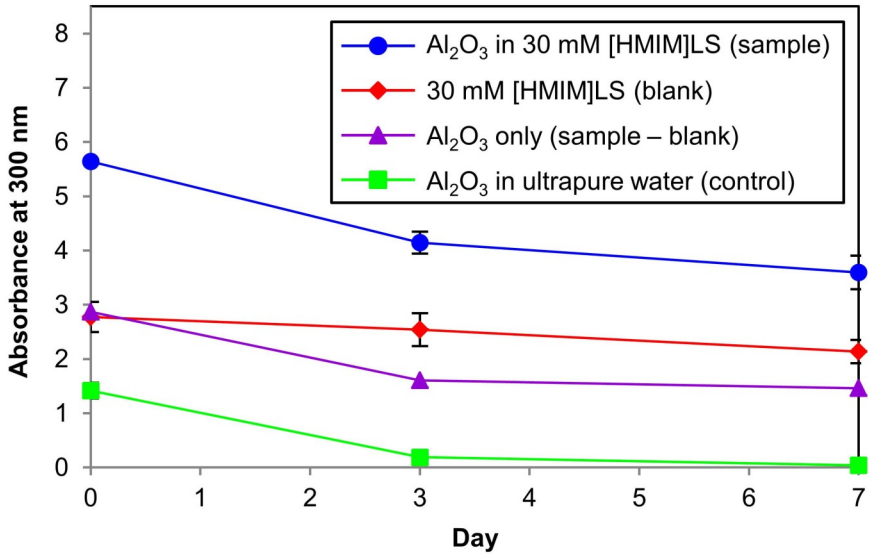

Figure 5. Absorbance at 300 nm of Al_2O-$_3$ nanofluids and aqueous [HMIM]LS solution from day 0 to day 7: () 300 ppm Al_2O_3 in 30 mM [HMIM]LS, (¿) 30 mM [HMIM]LS, and (¢) 300 ppm Al_2O_3 in ultrapure water. The plot for 300 ppm Al_2O_3 only (p) was determined by subtracting the absorbance of the blanks from the absorbance of the samples. Please note that the samples were diluted prior to any absorbance measurements within the detection limit of the equipment; absorbance values presented here were after multiplying the dilution factor.

Absorbance of the nanofluids was measured from 200 to 800 nm. In **Figure 4**, absorbance of the aqueous solution of [HMIM]LS was weak above 250 nm; thus, its effect on absorbance in this region was ignored. Based on this, absorbance at 300 nm was selected as a benchmark in comparing the stability of the nanofluids through time. **Figure 5** showed the plot of the absorbance of the samples, controls and blanks from Day 0 to Day 7 at this wavelength to depict the enhanced dispersion of the nanoparticles in the [HMIM]LS solution. The controls (¢) showed a decreasing trend from Day 0 to Day 7, which corresponded to a reduction in nanoparticle concentration to a negligible value. On the other hand, the absorbance of the samples () was consistently higher from Day 0 to Day 7 compared to both controls and blanks (¿). To obtain the absorbance of the Al_2O_3 nanoparticles only (p) in the samples, the absorbance of the blanks was subtracted from that of the samples. Again, the absorbance of Al_2O_3 only in the samples was consistently higher than the controls by a factor of 2, 9, and 38 from Day 0, Day 3, and Day 7, respectively. This consistent overlap of the absorption spectra of the samples to the spectra of the controls was indicative of the excellent stability of the nanofluids with the IL as dispersant [40]. Moreover, these results corroborated the sedimentation photographs shown in **Figure 3**.

Table 2. Analysis of variance: Effect of particle concentration, IL concentration and time elapsed on the absorbance of Al_2O_3 nanoflui

Transform: Square root		Constant: 0.056602				
Source	Sum of squares	Degrees of freedom	Mean square	F Value	p-value Prob > F	Remark
Model	21.51314	11	1.9557	474.8199	< 0.0001	significant
A – Particle concentration	2.057175	1	2.0572	499.4467	< 0.0001	
B – IL concentration	17.63014	1	17.6301	4280.2947	< 0.0001	
C – Time elapsed	1.002222	2	0.5011	121.6611	< 0.0001	
AB	0.020198	1	0.0202	4.9038	0.0365	
AC	0.603738	2	0.3019	73.2886	< 0.0001	
BC	0.040071	2	0.0200	4.8642	0.0168	
ABC	0.159589	2	0.0798	19.3728	< 0.0001	
Pure Error	0.098854	24	0.0041			
Cor Total	21.61199	35				

The Model F-value of 474.82 implies the model is significant. There is only a 0.01% chance that a "Model F-Value" this large could occur due to noise.

To check the statistical reliability of the results, analysis of variance on absorbance at 300 nm against the particle concentration, ionic liquid concentration and elapsed time was conducted (**Table 2**). The results of analysis showed that the data were statistically significant for the chosen model. The effect of IL concentration and its interaction with both particle concentration and elapsed time were significant. Therefore, based on the absorbance measurements, [HMIM]LS was an effective dispersant.

3.4 Zeta potential measurements and particle size distribution

Figure 6 shows the zeta potential measurements of nanofluids monitored within a 7-day period. The zeta potential of the controls (¢) was positively charged, which signified that the particle surface of Al_2O_3 was protonated [41, 46]. In terms of absolute value, the zeta potential of the control showed an increasing trend: 23.5 mV, 31.7 mV and 33.5 mV from Day 0, Day 3 and Day 7, respectively. These results indicated that the controls were moderately stable [32], which were contradictory to the absorbance measurements. However, zeta potential is an intrinsic property of a nanoparticle in a liquid [47]. The surface charge of the remaining colloidal particles still suspended in the controls might explain these readings. On the other hand, the zeta potential of the samples () was negatively charged which was similar to the zeta potential of the blanks (¿) at Day 0 as shown in **Figure 6**. In terms of absolute value, the zeta potential increased as well: -19.2 mV, -30.7 mV, and -36.9 mV for Day 0, Day 3 and Day 7, respectively. In contrast to the blanks, the zeta potential remained relatively constant (from -19 mV to -20 mV) throughout the testing period. It showed that the stability of Al_2O_3 in aqueous [HMIM]LS solution increased through time, from low stability (|15| mV < zeta potential < |30| mV) to moderate stability (|30| mV < zeta potential < |45| mV) [32]. Both the absorbance measurements and sedimentation photographs corroborated these zeta potential measurements.

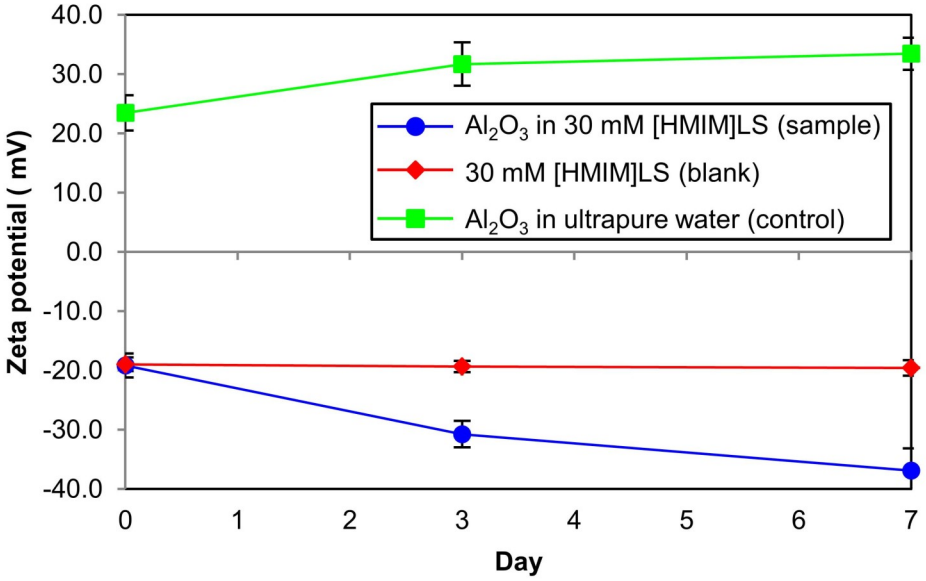

Figure 6. Zeta potential of Al_2O_{-3} nanofluids and aqueous [HMIM]LS solution from day 0 to day 7: () 300 ppm Al_2O_3 in 30 mM [HMIM]LS, (¿) 30 mM [HMIM]LS, and (¢) 300 ppm Al_2O_3 in ultrapure water.

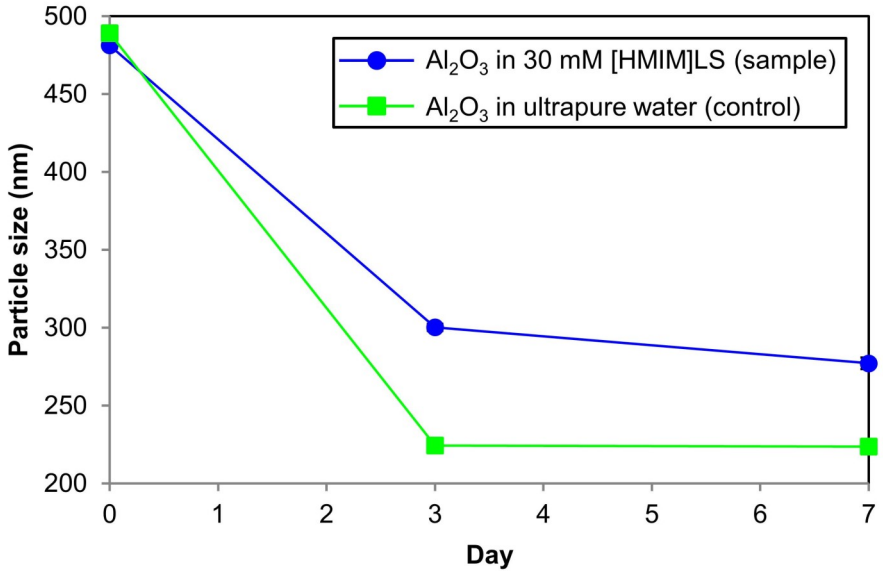

Figure 7. Mean particle size of 300 ppm Al_2O_{-3} nanoparticles in ultrapure water (¢) and 30 mM [HMIM]LS (), respectively, from day 0 to day 7.

Figure 7 shows the mean particle size in both the samples and controls through time. At Day 0, both the samples () and controls (¢) started out with similar mean particle size. But through time, the mean particle size of the controls rapidly decreased. This corresponded to the settling of larger aggregates as shown by the sudden narrowing of the particle size distribution plots of the controls in **Figure 8(a)**, **Figure 8(b)** and **Figure 8(c)**. On the other hand, the samples seemed to show a slower settling rate with a relatively higher mean particle size through time compared to the controls. The gradual narrowing of the particle size distribution plots of the samples as shown in **Figure 8(d)**, **Figure 8(e)** and **Figure 8(f)** corroborated these results. There were still some particles with sizes greater than 1000 nm detected on Day 7 as shown in **Figure 8(d)**. On the other hand, the peaks at sizes <100 nm corresponded to colloidal particles that will likely remain indefinitely suspended.

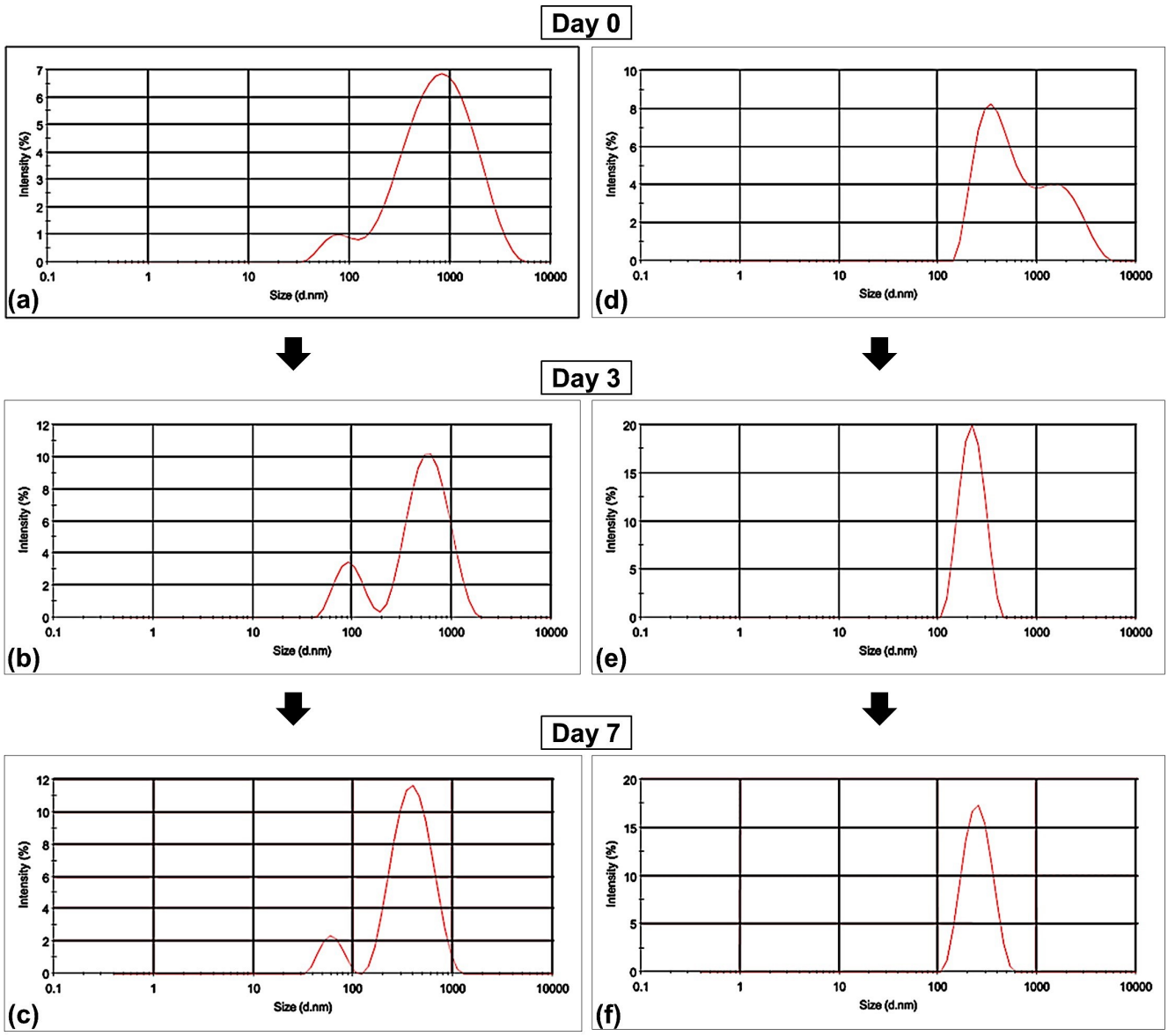

Figure 8. Particle size distribution plots of 300 ppm Al_2O_3 nanoparticles in 30 mM [HMIM]LS solution (a, b, c) and in ultrapure water (d, e, f), respectively, from day 0 to day 7.

Analyses of variance on zeta potential values and mean particle size were also performed. The results showed that the effect of IL on both the zeta potential and mean particle size was significant (**Table 3** and **Table 4**). Moreover, the interaction of [HMIM]LS with the nanoparticle concentration and interaction of [HMIM]LS with time were both significant. Therefore, it can be concluded that in terms of both zeta potential measurements and the particle size distribution, [HMIM]LS was an effective dispersant. The steric protection and electrostatic repulsion provided by the IL, as well as the increased viscosity of the IL solution, may retard the settling of particles including the larger agglomerated ones [10, 48].

Table 3. Analysis of variance: Effect of the particle concentration, [HMIM]LS concentration and elapsed time on the zeta potential of 300 ppm Al_2O_3 nanofluids.

Source	Sum of squares	Degrees of freedom	Mean square	F value	p-value Prob > F	Remark
Model	18611.46972	11	1691.952	357.4966	< 0.0001	significant
A-Particle Concentration	891.0225	1	891.0225	188.2663	< 0.0001	
B-IL Concentration	13607.2225	1	13607.22	2875.103	< 0.0001	
C-Time Elapsed	26.15055556	2	13.07528	2.762707	0.0832	
AB	3455.480278	1	3455.48	730.1167	< 0.0001	
AC	19.26166667	2	9.630833	2.034922	0.1526	
BC	319.0416667	2	159.5208	33.70554	< 0.0001	
ABC	293.2905556	2	146.6453	30.98503	< 0.0001	
Pure Error	113.5866667	24	4.732778			
Cor Total	18725.05639	35				
The Model F-value of 357.50 implies the model is significant. There is only a 0.01% chance that a "Model F-Value" this large could occur due to noise.						

Table 4. Analysis of variance: Effect of [HMIM]LS concentration and elapsed time on the particle size of 300 ppm nanofluids.

Transform: Power		Lambda: -2.05		Constant:0		
Source	Sum of squares	Degrees of freedom	Mean square	F value	p-value Prob > F	Remark
Model	4.34E-10	5	8.68E-11	1080.613	< 0.0001	significant
A-IL Concentration	7.09E-11	1	7.09E-11	882.8029	< 0.0001	
B-Elapsed Time	3.24E-10	2	1.62E-10	2017.522	< 0.0001	
AB	3.9E-11	2	1.95E-11	242.6097	< 0.0001	
Pure Error	9.64E-13	12	8.03E-14			
Cor Total	4.35E-10	17				
The Model F-value of 1080.61 implies the model is significant. There is only a 0.01% chance that a "Model F-Value" this large could occur due to noise.						

3.5 Discussion

The proposed mechanism for the effectivity of [HMIM]LS as dispersant to Al_2O_{-3} nanofluids may be attributed to the double layer micellar formation around the nanoparticles. Referring to another SAIL from the [RMIM]LS family, 1-butyl-3-methylimidazolium lauryl sulfate [BMIM]LS was also shown to control and stabilize the growth of synthesized gold nanoparticles. The bilayer formation around the nanoparticles provided both electrostatic repulsion and steric protection that prevented particle aggregation [27].

The double layer micellar formation in this study may be attributed to $[HMIM]^+$ cations mainly adsorbed on the oxide surface of Al_2O_{-3} by electrostatic interaction through tail-to-tail (hydrophobic) interaction of both

the $[HMIM]^+$ cations and lauryl sulfate anions facing the aqueous solution. Three pieces of evidence support this mechanism. First, the measured pH of the Al_2O_3/30 mM [HMIM]LS nanofluid was pH 2.32. A similar result was obtained in an adsorption study of 1-octyl-3-methylimidazolium chloride ([OMIM]Cl) by kaolinite, wherein the pH of the suspension decreased with increasing ionic liquid concentration [46]. It was suggested that adsorbed $[OMIM]^+$ cations replaced the hydrogen ions on the surface of the mineral forcing them back to the solution and resulted to the decrease in pH. Secondly, in the graph presented in **Figure 9**, peak absorbance of 30 mM [HMIM]LS solution was measured at 211 nm (). However, peak absorbance of [HMIM]LS in Al_2O_3 nanofluids was measured at 228 nm (£). The peak of the samples was red-shifted relative to the peak of the blanks which suggested the stabilizing effect of the IL i.e. $[HMIM]^+$ cations were in micelles around the particles. Similar findings in studies [27, 28] of IL-stabilized gold nanoparticles wherein red-shifting implied the ionic liquid's size-controlling capability. On the other hand, a blue shift had been reported for polypeptide IL-stabilized CNT-water dispersion that was attributed to the interaction between the ionic liquid and CNT surface [35]. Thirdly, the negative zeta potential measured indicating the net charge was mainly by the lauryl sulfate ions facing the solution. Partial charge neutralization of the interaction between the positive imidazolium ring and negative oxygen of the lauryl sulfate ion had been ascribed to the negative zeta potential values of mixtures of imidazolium ILs and SLS [49]. In addition, the relatively low absolute value of the zeta potential measured may also be attributed to an adsorbed layer of the IL that shifted the plain of shear, at which the zeta potential was measured, to a larger distance from the particle surface. Nevertheless, the steric stabilization in combination with electrostatic repulsion at this zeta potential still rendered the system stable [50].

For double layer micellar stabilization to be effective, the dispersant should be set above the CMC so that there is maximum surface coverage by the ionic liquid [41]. In this study, ionic liquid concentration was set relatively higher than the CMC since nanoparticles have the tendency to shift it to a higher concentration [42]. However, a high ionic liquid concentration may have a drawback. Since micelle formation around nanoparticles and in bulk solution compete with each other; at high concentrations, the IL may have preferred the latter to reach a desired equilibrium [33]. With the eventual decrease of IL available for double layer micellar stabilization, some aggregation and settling of the nanoparticles may have occurred. An evidence of the gradual return of IL to the bulk solution was shown in **Figure 9**; wherein, the intensity of the peak absorbance for Al_2O_3-water with [HMIM] LS nanofluids (—) increased from Day 0 to Day 7. Nevertheless, high consideration of the surfactant's CMC must be given to prevent rapid settling of the nanoparticles [14, 15].

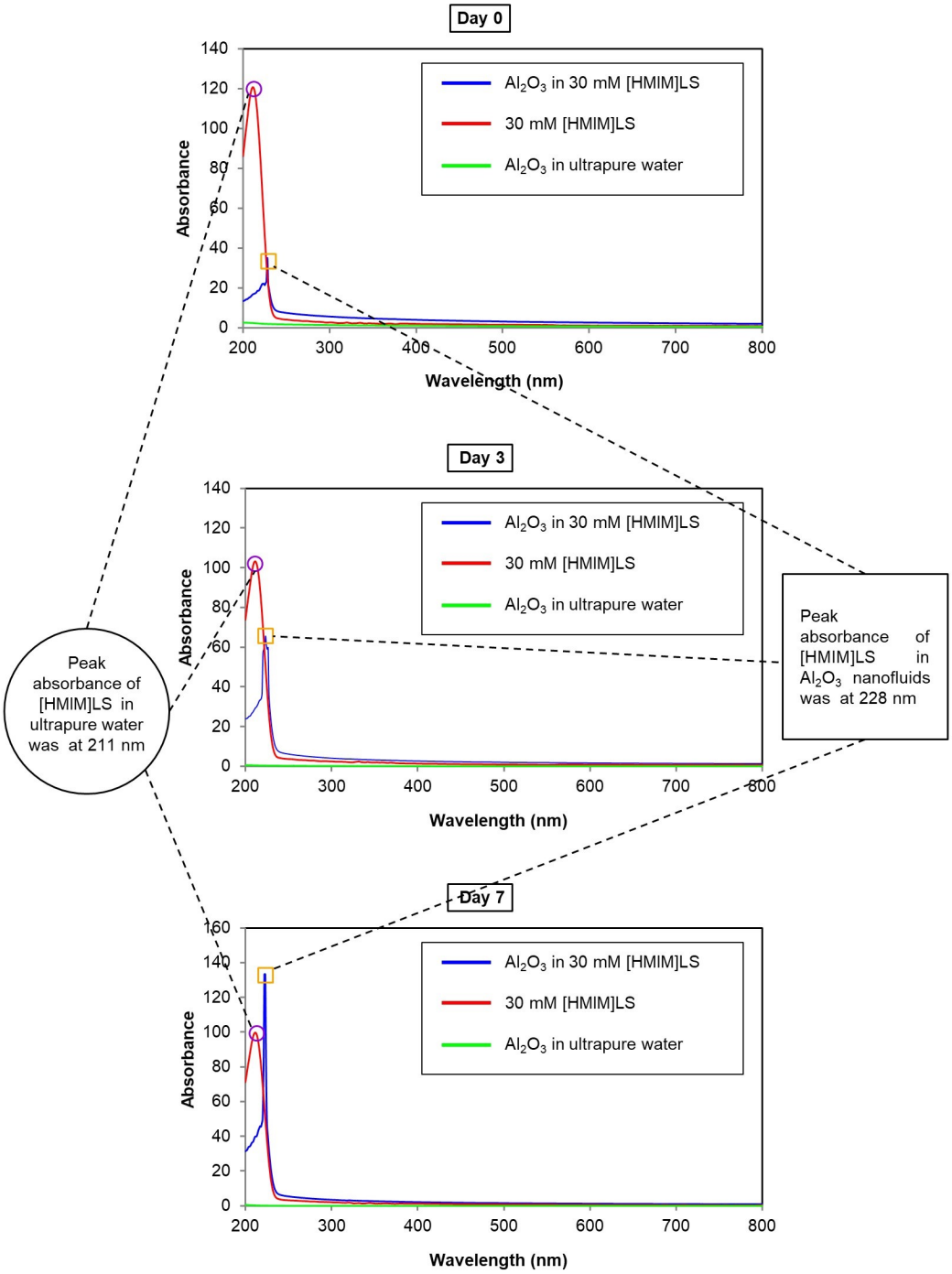

Figure 9. Peak absorbance of [HMIM]LS in ultrapure water and [HMIM]LS in Al_2O_3-water nanofluids. Please note that the samples were diluted prior to any absorbance measurements within the detection limit of the equipment; absorbance values presented here were after multiplying the dilution factor.

Thermodynamically, a system with particles in constant Brownian motion tended to move towards an aggregated, phase-separated condition [12]. However, particles must be able to overcome an energy barrier in order to aggregate during collisions [12, 13]. The higher the energy barrier, the less likely they aggregated, therefore the more stable the system. Manipulation of the energy barrier may be done through surface chemical effect, the addition of dispersant or both [10]. In this study, the IL may have provided enough repulsive force to raise that energy barrier preventing most of the nanoparticles from aggregating.

Besides the steric protection and electrostatic repulsion provided by the IL, the increased viscosity of IL solutions [51] may also be attributed to the retarded settling of the nanoparticles. It was noted that the settling rate of particles was inversely proportional to the viscosity of the host fluid. Thus, this suggested that the nanofluids with IL dispersant were relatively more stable [10, 48].

IV. CONCLUSION

The findings of this study showed that [HMIM]LS, a low cost and "greener" surface-active ionic liquid derived from sodium lauryl sulfate, was an effective dispersant of Al_2O_3 nanoparticles in water. In the one-week colloidal stability test conducted, absorbance, zeta potential and particle size measurements corroborated the hindered aggregation and settling of the nanoparticles. Analyses of variance on the results, showed that [HMIM]LS had a significant role to the enhanced colloidal stability. Visual monitoring through sedimentation photographs taken over a month supported that Al_2O_3 nanoparticles in water with [HMIM]LS have better long-term colloidal stability. There were also additional supporting pieces of evidence for double layer micellar mechanism by the IL around the nanoparticles that provided both steric protection and electrostatic repulsion preventing nanoparticle aggregation. However, the increased viscosity of IL aqueous solutions can be attributed to the retarded nanoparticle settling. From these encouraging results, future studies may delve into the following: further verification of the IL-aluminum oxide interaction through electron microscopy and infrared spectroscopy; the determination of the ideal agitation and/or sonication times as the optimal ratio of nanoparticle volume fraction to the IL concentration; and comparative experiments of the IL's performance as surfactant to industry standards for practical applications.

V. ACKNOWLEDGEMENTS

The authors gratefully acknowledge the financial support given by the Department of Science and Technology, Government of the Republic of the Philippines through the Engineering Research and Development for Technology Program. They also extend their gratitude to the faculty and laboratory staff of the Energy Engineering Program, the Department of Chemical Engineering, the Institute of Chemistry, and the National Sciences Research Institute of the University of the Philippines, Diliman for their technical expertise, the use of facilities, and assistance.

References

[1] R. Taylor *et al.*, "Small particles, big impacts: A review of the diverse applications of nanofluids," *Journal of Applied Physics,* Article vol. 113, no. 1, pp. 011301-011301-19, 2013.

[2] M. Gupta, V. Singh, R. Kumar, and Z. Said, "A review on thermophysical properties of nanofluids and heat transfer applications," *Renewable and Sustainable Energy Reviews,* vol. 74, pp. 638-670, 2017/07/01/ 2017.

[3] W.-g. Kim, H. U. Kang, K.-m. Jung, and S. H. Kim, "Synthesis of Silica Nanofluid and Application to CO2 Absorption," *Separation Science and Technology,* vol. 43, no. 11-12, pp. 3036-3055, 2008/08/08 2008.

[4] T. P. Otanicar, P. E. Phelan, R. S. Prasher, G. Rosengarten, and R. A. Taylor, "Nanofluid-based direct absorption solar collector," *Journal of Renewable and Sustainable Energy,* vol. 2, no. 3, p. 033102, 2010.

[5] G. D. Dice, S. Mujumdar, and A. Y. Elezzabi, "Plasmonically enhanced diffusive and subdiffusive metal nanoparticle-dye random laser," *Applied Physics Letters,* vol. 86, no. 13, p. 131105, 2005.

[6] S. Nie, Y. Xing, G. J. Kim, and J. W. Simons, "Nanotechnology Applications in Cancer," *Annual Review of Biomedical Engineering,* vol. 9, no. 1, pp. 257-288, 2007/08/15 2007.

[7] D. Li, W. Fang, H. Wang, C. Gao, R. Zhang, and K. Cai, "Gold/Oil Nanofluids Stabilized by a Gemini Surfactant and Their Catalytic Property," *Industrial & Engineering Chemistry Research,* vol. 52, no. 24, pp. 8109-8113, 2013/06/19 2013.

[8] S. C. Roy, O. K. Varghese, M. Paulose, and C. A. Grimes, "Toward Solar Fuels: Photocatalytic Conversion of Carbon Dioxide to Hydrocarbons," *ACS Nano,* vol. 4, no. 3, pp. 1259-1278, 2010/03/23 2010.

[9] V. Fuskele and R. M. Sarviya, "Recent developments in Nanoparticles Synthesis, Preparation and Stability of Nanofluids," *Materials Today: Proceedings,* vol. 4, no. 2, pp. 4049-4060, 2017/01/01/ 2017.

[10] A. Ghadimi, R. Saidur, and H. S. C. Metselaar, "A review of nanofluid stability properties and characterization in stationary conditions," *International Journal of Heat and Mass Transfer,* vol. 54, no. 17–18, pp. 4051-4068, 8// 2011.

[11] K. H. Solangi *et al.*, "A comprehensive review of thermo-physical properties and convective heat transfer to nanofluids," *Energy,* vol. 89, pp. 1065-1086, 9// 2015.

[12] T. Cosgrove, *Colloid science. principles, methods and applications*. United Kingdom: Wiley: A John Wiley and Sons, Ltd, Publication, 2010.

[13] S. M. Peker and S. S. Helavcı, *Solid-liquid two phase flow*. Amsterdam, The Netherlands: Elsevier, 2008.

[14] N. A. C. Sidik, H. A. Mohammed, O. A. Alawi, and S. Samion, "A review on preparation methods and challenges of nanofluids," *International Communications in Heat and Mass Transfer,* vol. 54, pp. 115-125, 5// 2014.

[15] Z. Haddad, C. Abid, H. F. Oztop, and A. Mataoui, "A review on how the researchers prepare their nanofluids," *International Journal of Thermal Sciences,* vol. 76, pp. 168-189, 2// 2014.

[16] W. Yu and H. Xie, "A review on nanofluids: preparation, stability mechanisms, and applications," *J. Nanomaterials,* vol. 2012, pp. 1-17, 2012.

[17] K. S. Suganthi and K. S. Rajan, "Metal oxide nanofluids: Review of formulation, thermo-physical properties, mechanisms, and heat transfer performance," *Renewable and Sustainable Energy Reviews,* vol. 76, pp. 226-255, 2017/09/01/ 2017.

[18] J. Jiao *et al.*, "Aggregation Behaviors of Dodecyl Sulfate-Based Anionic Surface Active Ionic Liquids in Water," *The Journal of Physical Chemistry B,* vol. 116, no. 3, pp. 958-965, 2012/01/26 2012.

[19] I. H. J. Arellano, J. G. Guarino, F. U. Paredes, and S. D. Arco, "Thermal stability and moisture uptake of 1-alkyl-3-methylimidazolium bromide," (in English), *Journal of Thermal Analysis and Calorimetry,* vol. 103, no. 2, pp. 725-730, 2011/02/01 2011.

[20] H. Olivier-Bourbigou, L. Magna, and D. Morvan, "Ionic liquids and catalysis: Recent progress from knowledge to applications," *Applied Catalysis A: General,* vol. 373, no. 1–2, pp. 1-56, 1/31/ 2010.

[21] B. Dong, X. Zhao, L. Zheng, J. Zhang, N. Li, and T. Inoue, "Aggregation behavior of long-chain imidazolium ionic liquids in aqueous solution: Micellization and characterization of micelle microenvironment," *Colloids and Surfaces A: Physicochemical and Engineering Aspects,* vol. 317, no. 1–3, pp. 666-672, 3/20/ 2008.

[22] J. M. Obliosca, S. D. Arco, and M. H. Huang, "Synthesis and Optical Properties of 1-Alkyl-3-Methylimidazolium Lauryl Sulfate Ionic Liquids," (in English), *Journal of Fluorescence,* vol. 17, no. 6, pp. 613-618, 2007/11/01 2007.

[23] R. Saidur, K. Y. Leong, and H. A. Mohammad, "A review on applications and challenges of nanofluids," *Renewable and Sustainable Energy Reviews,* vol. 15, no. 3, pp. 1646-1668, 4// 2011.

[24] V. Sridhara and N. Satapathy Lakshmi, "Al2O3-based nanofluids: a review," *Nanoscale Research Letters,* Journal article no. 1, p. 456, 2011.

[25] A. Modaressi, A. Boulmokh, F. Mutelet, U. Domańska, I. Bąkała, and M. Rogalski, "Extracting capacity of ionic liquids adsorbed at the surface of alumina nanoparticles: Conductimetric and dynamic light scattering studies," *Colloids and Surfaces A: Physicochemical and Engineering Aspects,* vol. 338, no. 1–3, pp. 47-50, 4/15/ 2009.

[26] J. M. Obliosca, I. H. J. Arellano, M. H. Huang, and S. D. Arco, "Morphogenesis of anistropic nanostructures stabilized by the greener ionic liquid 1-butyl-3-methylimidazolium lauryl sulphate," *Philippine Science Letters,* vol. 3, pp. 121–127, 2010.

[27] J. M. Obliosca, I. H. J. Arellano, M. H. Huang, and S. D. Arco, "Double layer micellar stabilization of gold nanocrystals by greener ionic liquid 1-butyl-3-methylimidazolium lauryl sulfate," *Materials Letters,* vol. 64, no. 9, pp. 1109-1112, 5/15/ 2010.

[28] B. Wang, X. Wang, W. Lou, and J. Hao, "Gold-ionic liquid nanofluids with preferably tribological properties and thermal conductivity," *Nanoscale Research Letters,* vol. 6, no. 259, pp. 1-10, 2011.

[29] H. Zhang, H. Cui, S. Yao, K. Zhang, H. Tao, and H. Meng, "Ionic liquid-stabilized non-spherical gold nanofluids synthesized using a one-step method," *Nanoscale Research Letters,* vol. 7, no. 583, pp. 1-8, 2012.

[30] A. Di Crescenzo *et al.*, "Disaggregation of single-walled carbon nanotubes (SWNTs) promoted by the ionic liquid-based surfactant 1-hexadecyl-3-vinyl-imidazolium bromide in aqueous solution," *Soft Matter,* 10.1039/B812022F vol. 5, no. 1, pp. 62-66, 2009.

[31] X. Zhou, T. Wu, K. Ding, B. Hu, M. Hou, and B. Han, "The dispersion of carbon nanotubes in water with the aid of very small amounts of ionic liquid," *Chemical Communications,* 10.1039/B900849G no. 14, pp. 1897-1899, 2009.

[32] L. Vandsburger, "Synthesis and covalent surface modification of carbon nanotubes for preparation of stabilized nanofluid suspensions," Master of Engineering, Department of Chemical Engineering, McGill University, Canada, Master of Engineering, 2009.

[33] Y. Liu, L. Yu, S. Zhang, J. Yuan, L. Shi, and L. Zheng, "Dispersion of multiwalled carbon nanotubes by ionic liquid-type Gemini imidazolium surfactants in aqueous solution," *Colloids and Surfaces A: Physicochemical and Engineering Aspects,* vol. 359, no. 1–3, pp. 66-70, 4/20/ 2010.

[34] B. Dong, Y. Su, Y. Liu, J. Yuan, J. Xu, and L. Zheng, "Dispersion of carbon nanotubes by carbazole-tailed amphiphilic imidazolium ionic liquids in aqueous solutions," *Journal of Colloid and Interface Science,* vol. 356, no. 1, pp. 190-195, 4/1/ 2011.

[35] Q. Hu, Y. Deng, Q. Yuan, Y. Ling, and H. Tang, "Polypeptide ionic liquid: Synthesis, characterization, and application in single-walled carbon nanotube dispersion," *Journal of Polymer Science Part A: Polymer Chemistry,* vol. 52, no. 2, pp. 149-153, 2014.

[36] C. Jungnickel, J. Łuczak, J. Ranke, J. F. Fernández, A. Müller, and J. Thöming, "Micelle formation of imidazolium ionic liquids in aqueous solution," *Colloids and Surfaces A: Physicochemical and Engineering Aspects,* vol. 316, no. 1–3, pp. 278-284, 3/5/ 2008.

[37] A. Beyaz, W. S. Oh, and V. P. Reddy, "Ionic liquids as modulators of the critical micelle concentration of sodium dodecyl sulfate," *Colloids and Surfaces B: Biointerfaces,* vol. 35, no. 2, pp. 119-124, 5/15/ 2004.

[38] T. Inoue, H. Ebina, B. Dong, and L. Zheng, "Electrical conductivity study on micelle formation of long-chain imidazolium ionic liquids in aqueous solution," *Journal of Colloid and Interface Science,* vol. 314, no. 1, pp. 236-241, 10/1/ 2007.

[39] R. Sadeghi, S. G. Etemad, E. Keshavarzi, and M. Haghshenasfard, "Investigation of alumina nanofluid stability by UV–vis spectrum," (in English), *Microfluidics and Nanofluidics,* vol. 18, no. 5-6, pp. 1023-1030, 2015/05/01 2015.

[40] F. Yu *et al.*, "Dispersion stability of thermal nanofluids," *Progress in Natural Science: Materials International,* vol. 27, no. 5, pp. 531-542, 2017/10/01/ 2017.

[41] B. Kasprzyk-Hordern, "Chemistry of alumina, reactions in aqueous solution and its application in water treatment," *Advances in Colloid and Interface Science,* vol. 110, no. 1–2, pp. 19-48, 6/30/ 2004.

[42] C. R. Evanko, D. A. Dzombak, and J. W. Novak Jr, "Influence of surfactant addition on the stability of concentrated alumina dispersions in water," *Colloids and Surfaces A: Physicochemical and Engineering Aspects,* vol. 110, no. 3, pp. 219-233, 5/24/ 1996.

[43] K. Esumi, M. Iitaka, and K. Torigoe, "Kinetics of Simultaneous Adsorption of Poly(vinylpyrrolidone) and Sodium Dodecyl Sulfate on Alumina Particles," *Journal of Colloid and Interface Science,* vol. 232, no. 1, pp. 71-75, 12/1/ 2000.

[44] H. Jonggan, K. Sang Hyun, and K. Dongsik, "Effect of laser irradiation on thermal conductivity of ZnO nanofluids," *Journal of Physics: Conference Series,* vol. 59, no. 1, p. 301, 2007.

[45] Y. Hwang *et al.*, "Stability and thermal conductivity characteristics of nanofluids," *Thermochimica Acta,* vol. 455, no. 1–2, pp. 70-74, 4/1/ 2007.

[46] M. Markiewicz, W. Mrozik, K. Rezwan, J. Thöming, J. Hupka, and C. Jungnickel, "Changes in zeta potential of imidazolium ionic liquids modified minerals – Implications for determining mechanism of adsorption," *Chemosphere,* vol. 90, no. 2, pp. 706-712, 1// 2013.

[47] F. Wypych and K. G. Satyanarayana, *Clay Surfaces: Fundamentals and Applications*. The Netherlands: Elsevier, Ltd., 2004.

[48] C. J. Geankoplis, *Principles of transport processes and separation technologies*. New Jersey, USA: Pearson Education, Inc., , 2005.

[49] S. Javadian, F. Nasiri, A. Heydari, A. Yousefi, and A. A. Shahir, "Modifying Effect of Imidazolium-Based Ionic Liquids on Surface Activity and Self-Assembled Nanostructures of Sodium Dodecyl Sulfate," *The Journal of Physical Chemistry B,* vol. 118, no. 15, pp. 4140-4150, 2014/04/17 2014.

[50] C. M. Keck, "Cyclosporine Nanosuspensions: Optimised Size Characterisation & Oral Formulations " Doctor of Science (Dr. rer. Nat.) Doctoral, Department of Biology, Chemistry and Pharmacy, Freie Universität Berlin, Germany, 2006.

[51] T. Singh and A. Kumar, "Thermodynamics of dilute aqueous solutions of imidazolium based ionic liquids," *The Journal of Chemical Thermodynamics,* vol. 43, no. 6, pp. 958-965, 6// 2011.